Moving forward: A review of continuous kinetics and kinematics during wheelchair and handcycling propulsion

Kellie M. Halloran[a], Michael D. K. Focht[a], Alexander Teague[b], Joseph Peters[c,d], Ian Rice[e], Mariana E. Kersh[a,b,c,*]

[a]*Department of Mechanical Science and Engineering, University of Illinois Urbana-Champaign*
[b]*Carle Illinois College of Medicine, University of Illinois Urbana-Champaign*
[c]*Beckman Institute for Advanced Science and Technology, University of Illinois Urbana-Champaign*
[d]*Disability Resources and Educational Services, University of Illinois Urbana-Champaign*
[e]*Department of Kinesiology, University of Illinois Urbana-Champaign*

Abstract

Wheelchair users (WCUs) face high rates of shoulder overuse injuries. As exercise is recommended to reduce cardiovascular disease prevalent among WCUs, it is becoming increasingly important to understand the mechanisms behind shoulder soft-tissue injury in WCUs. Understanding the kinetics and kinematics during upper-limb propulsion is the first step toward evaluating soft-tissue injury risk in WCUs. This paper examines continuous kinetic and kinematic data available in the literature. Two everyday modes (everyday wheelchair use and attach-unit handcycling) are examined, as well as two athletic modes (wheelchair racing and recumbent handcycling). These athletic modes are important considering the higher contact forces, speed, and power outputs experienced during these activities that could be putting users at increased risk of injury. Understanding the underlying kinetics and kinematics during various propulsion modes can lend insight into shoulder loading, and therefore injury risk, during these activities and inform future exercise guidelines for WCUs.

Keywords: exercise, propulsion, shoulder, handrim, handcrank

1. Introduction

In the United States, an estimated 5.5 million people rely on wheelchairs as their primary means of locomotion(Taylor, 2018) due to a variety of conditions including congenital defects, spinal cord injuries, movement disorders, and stroke(Taylor, 2018, Karmarkar et al., 2011). As mobility impairments are often permanent, wheelchair users (WCUs) depend on their wheelchairs and upper extremities for ambulation.

Unfortunately, the transition to wheelchair use and increase in shoulder loading cycles as a result of wheelchair-related activities places the upper extremity at increased risk for injury(Burnham et al., 1993, Subbarao et al., 1995, Jahanian et al., 2020, Gill et al., 2014, Hinrichs et al., 2016). 40-75% of WCUs report upper extremity injury and pain, often at the shoulder(Dalyan et al., 1999, Alm et al., 2008, Curtis and Dillon, 1985, Finley et al., 2004), which is attributed to overuse from wheelchair propulsion and transfers (Barber and Gall, 1991). The increased loading of the upper arm is suggested to result in degenerative morphological changes in the shoulder soft tissue (Brose et al., 2008), rotator cuff impingement (Bayley et al., 1987), and rotator cuff tendinopathy (Jahanian et al., 2020, Gill et al., 2014, Lal, 1998).

These high rates of shoulder pain are one of many factors contributing to reduced exercise rates in WCUs(Hansen et al., 2021). Despite clear evidence supporting the benefits of exercise, engagement in exercise is low in WCUs due to socioecological, institutional, physical, and interpersonal challenges(Kehn and Kroll,

*Corresponding author: mkersh@illinois.edu (Mariana E. Kersh)

2009, Gorgey, 2014). Physical inactivity in WCUs increases the rates of obesity, diabetes, hypertension, and dyslipidemia (Gater et al., 2019, Barry et al., 2013), which are major risk factors for cardiovascular disease (CVD).

Adaptive sports, which have grown in popularity among WCUs in recent years(Heyward et al., 2017), are known to be both physically and psychologically beneficial for people with disabilities(Blauwet and Willick, 2012) and thus present an opportunity to improve cardiovascular function, psychological health, and overall quality of life for WCUs. From a biomechanical perspective, because shoulder function is of paramount importance to WCU populations, it is essential that these sports and exercises do not contribute to or worsen upper limb pain.

Manual wheelchair users have very few choices for accumulating cardiovascular exercise through the upper limbs. Therefore, it becomes imperative to optimize known activities for safety and benefits. While it is clear that athletes have the potential to experience elevated forces and moments during athletic propulsion modes, a nuanced approach must be employed to understand injury susceptibility. For example, body position, stroke timing characteristics, hand interface, muscle activation patterns, and involved muscle groups differ considerably by sport. In essence, body position variations may affect how forces are received and handled by the soft tissues of the upper limb during propulsion.

Our understanding of shoulder function can be informed by computational methods that combine in vivo biomechanical data (kinematics, kinetics) with musculoskeletal models of the body. One modeling technique involves the use of rigid-body systems based on subject anthropometrics to simulate different tasks using collected kinematic and kinetic data. The outputs of rigid-body dynamics models include joint accelerations, joint torques, muscle forces, and joint contact forces(Faber et al., 2018, Martinez et al., 2020, Wu et al., 2016, Veeger et al., 2002). When combined with computational models at the tissue level, it is possible to obtain estimates of strains. Such models have been used to evaluate rotator cuff tears (Inoue et al., 2013, Redepenning et al., 2020), and have the potential to determine whether a given exercise type may or may not place the shoulder at risk of injury.

Critical to computational analyses of shoulder biomechanics during wheelchair usage is the underlying kinematic and kinetic data used as input to these models. As such, the purpose of this review is to summarize existing literature reporting continuous (time-series) kinetic and kinematic data during handrim and crank propulsion - two common modes of locomotion used by WCUs. Within this review, we first describe our methodology for selection of papers and data reduction (Section 2). Next, we summarized kinematic and kinetic data for two types of propulsion: handrim (Section 3) and crank (Section 4). Within each propulsion type we compared everyday usage to athletic forms.

2. Methods

Retrieval of papers was performed using Google Scholar and Pubmed with combinations of the following keywords: "Wheelchair", "Kinetics", "Kinematics", "Forces", "Handcycle", and "Inverse Dynamics". Forward and backward citation searches were used to find additional studies. Studies reporting kinematic and applied force data were included if the authors reported time-series data over the course of a propulsion cycle. Studies reporting discrete (single time point) kinetic or kinematics data were excluded. Studies reporting force data in the global x,y,z coordinate system but not the tangential, radial, and lateral components were also excluded. In the 1990s, most racers shifted from an upright sitting position to a forward, crouched position (Vanlandewijck et al., 2001). Thus, racing wheelchair propulsion studies published before 1990 were excluded from this review.

For the purposes of this review, we report force data using polar conventions. Tangential force, the force parallel to the wheel or crank path, is positive when in the direction of rotation. Positive radial force was defined as the force pointing towards the center of the wheel or center of handcycle rotation, and laterally oriented forces orthogonal to the sagittal plane were defined as positive.

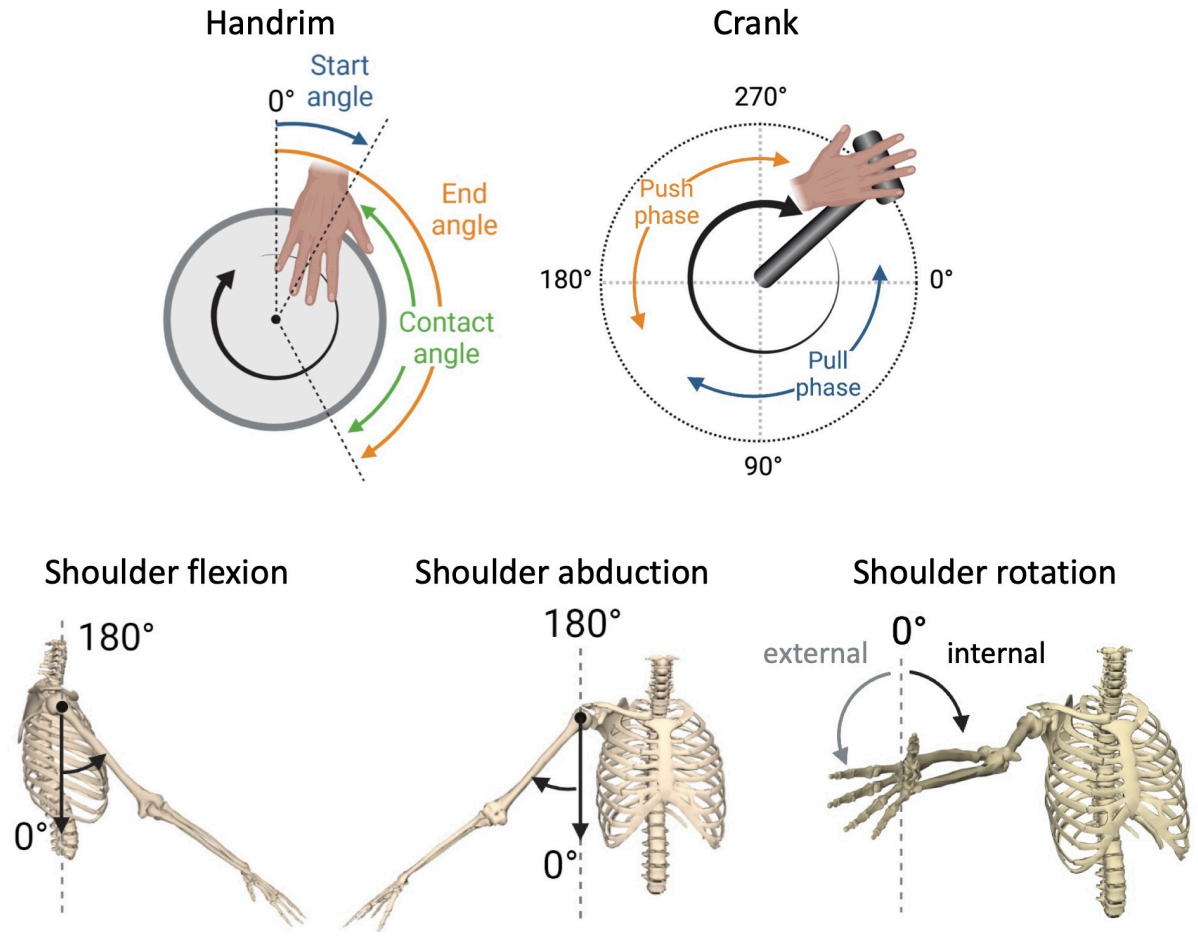

Figure 1: **Top** Handrim (left) and crank (right) propulsion angle conventions (right-hand side). Note that in handrim propulsion 0° is at the top of the wheel, while in handcycling 0° is furthest away from the user. **Bottom** Shoulder angles definitions based on the flexion/abduction/rotation angle set(Anglin and Wyss, 2000). Note that the rotation angle is referencing rotation of the humerus.

Continuous (time-series) kinematic or kinetic data from published figures were digitized using WebPlotDigitizer. At least 15 data points were digitized per plot. Data were processed in MATLAB and Microsoft Excel. For handrim propulsion, only data during the push-phase was analyzed and was normalized by length of push phase. 0° positions for both propulsion modes followed literature conventions (Fig 1).

Joint angle descriptions in the literature consistently followed the flexion/abduction/rotation set of shoulder rotations (Fig 1)(Anglin and Wyss, 2000). All angles refer to the position of the scapula relative to the humerus. To allow for direct comparisons between studies, only studies that reported joint angles following these conventions were digitized and included in this review.

When multiple propulsion cycles were reported per test condition (e.g. same speed, PO, or trial), each cycle was digitized and the cycles were averaged to obtain a representative curve from the test condition. In some cases, data from multiple studies were combined using a weighted average based on the number of study participants. All figures were rendered in R (v4.0.5).

3. Handrim Propulsion

A propulsion cycle for everyday wheelchair propulsion involves grabbing the handrim and pushing followed by a hand recovery path where no handrim contact occurs(Vanlandewijck et al., 2001). While some exercise can be done in an upright wheelchair, WCUs switch from an everyday wheelchair to racing wheelchairs to achieve

faster speeds. Rather than two smaller wheels, racing wheelchairs have one medium-sized wheel in the front which improves the chair's aerodynamics and enables higher speeds (Cooper and Luigi, 2014). Racing wheelchairs are propelled in a crouched kneeling position, with the user leaning forward compared to the upright sitting position of everyday wheelchair propulsion. Instead of grabbing the handrim, propulsion occurs with an individual "punching" the handrim, usually with a glove or hard hand-held implement(Cooper and Luigi, 2014).

In both handrim propulsion modes, the kinematics are split into two phases: the push phase, when the hand is in contact with the wheel rim, and the recovery phase, when the hand is in the air. The length of the push phase corresponds to the magnitude of the contact angle defined as the end angle minus the start angle (Fig 1).

3.1. Everyday Wheelchairs: Handrim Kinetics

With the development of the SmartWheel in the 1990's, it became feasible to record three-dimensional handrim forces during wheelchair propulsion and provide insight into loading of the upper extremity. To our knowledge, three studies have reported continuous tangential, radial, or lateral handrim force components during everyday wheelchair use(Boninger et al., 1997, Dallmeijer et al., 1998, Robertson et al., 1996). The maximum tangential forces ranged from 29 to 108 N (Fig 2A) and are on average greater than the range of maximum radial forces (36-40 N, Fig 2B) or lateral forces (19-33 N, Fig 2C). Tangential forces have a single peak in the last half of the push phase (54-79%) whereas radial and lateral forces have multiple peaks. Radial forces tend to reach a maximum early in the push phase (14-22%). In contrast, lateral forces tend to have two peaks: an initial lower peak in the first half of the push phase (12-27%) followed by a higher peak in the second half of the push phase (63-78%).

Differences in the magnitude of the tangential forces may be due to different wheelchair configurations and speeds used during testing. For example, the largest reported tangential forces occurred with subjects propelling at 60-80% of peak power outputs(Dallmeijer et al., 1998) while the other force profiles likely occurred at lower speeds (range: 1.5-2.0 m/s) (Robertson et al., 1996, Boninger et al., 1997). Experienced wheelchair users tended to apply lower peak tangential forces ($p=0.0001$) and took longer to reach the peak tangential forces ($p=0.0015$) than able-bodied participants (Robertson et al., 1996), though one exception is reported from Dallmeijer and colleagues (Dallmeijer et al., 1998).

Notably, the lateral force component reported from a subject with tetraplegia(Dallmeijer et al., 1998) was negative and with a single peak while others report positive double-peaked lateral forces. Whether or not the location and severity of spinal cord injury affects the loads applied during propulsion remains to be clearly demonstrated, but these data suggest that care should be taken when interpreting wheelchair kinetics from participants of varying injury levels.

3.2. Wheelchair Racing: Handrim Kinetics

An examination of the studies that report continuous applied forces during racing wheelchair propulsion(Chénier et al., 2021, Goosey-Tolfrey et al., 2001, Limroongreungrat et al., 2009, Miyazaki et al., 2020) yields results with high variability in both the shape of the force curves and the location of peak forces (Fig 2D-F). In contrast to everyday wheelchair usage, the maximum forces were applied radially during racing wheelchair propulsion. As expected due to increased speeds, the average maximum applied forces during racing propulsion were larger for all magnitudes of components compared to everyday propulsion (118 vs. 64 N for tangential forces, 251 vs. 38 N for radial forces, and 94 vs 26 N for lateral forces in racing vs. everyday propulsion, respectively). The maximum tangential forces (range: 105-131 N, Fig 2D) during racing propulsion peaks once in the middle of the push phase (40-69%) compared to the latter part of the push phase during wheelchair propulsion.

Similar to everyday propulsion, radial forces during racing peaked multiple times with maximum forces ranging from 150-428 N,

but all force profiles peaked in the second half of the push phase (64-82%) compared to earlier peaks at the beginning of the push phase for everyday propulsion (Fig 2E). Chenier et al. reported maximum radial forces of 427 N, which they attribute to the design of the force measurement system and the fact that their participant was propelling at maximum speed (Chénier et al., 2021). In contrast to everyday propulsion, two of the three racing studies reported negative lateral forces but with inconsistent force profiles. The positive lateral forces reported by Limroongreungrat et al. were attributed to differences in wheelchair design and propulsion speed(Limroongreungrat et al., 2009).

3.3. Everyday Wheelchairs: Kinematics

Kinematic profiles of the shoulder within the two studies reporting shoulder angles using the flexion/abduction/rotation conventions were consistent(Collinger et al., 2008, Rao et al., 1996). Collinger et al. reported mean shoulder angles for propulsion speeds of 0.9 and 1.8 m/s(Collinger et al., 2008), and Rao et al. reported mean shoulder angles for all subjects, who propelled with velocities ranging from 1.08 to 1.88 m/s. Wheelchair propulsion begins with the shoulder abducted to 53°, flexed to 48°, and internally rotated by 83°(Fig 3A-C, respectively). During the push phase, the shoulder adducts to 30°, extends to -12°, and internally rotates to 19°.

Boninger et al.(Boninger et al., 1998) and Koontz et al.(Koontz et al., 2002) also reported continuous shoulder angles but used projections of the humerus in the anatomical planes rather than the traditional shoulder joint angles. As a result, these shoulder angles were not included in our analysis as they cannot be compared to the other studies graphically, but they are worth noting as a source of continuous kinematic data.

3.4. Wheelchair Racing: Kinematics

Few studies have reported continuous joint angle data during racing propulsion using the current (post-1990's) racing wheelchair design. To our knowledge, the two studies that have reported continuous joint angles were

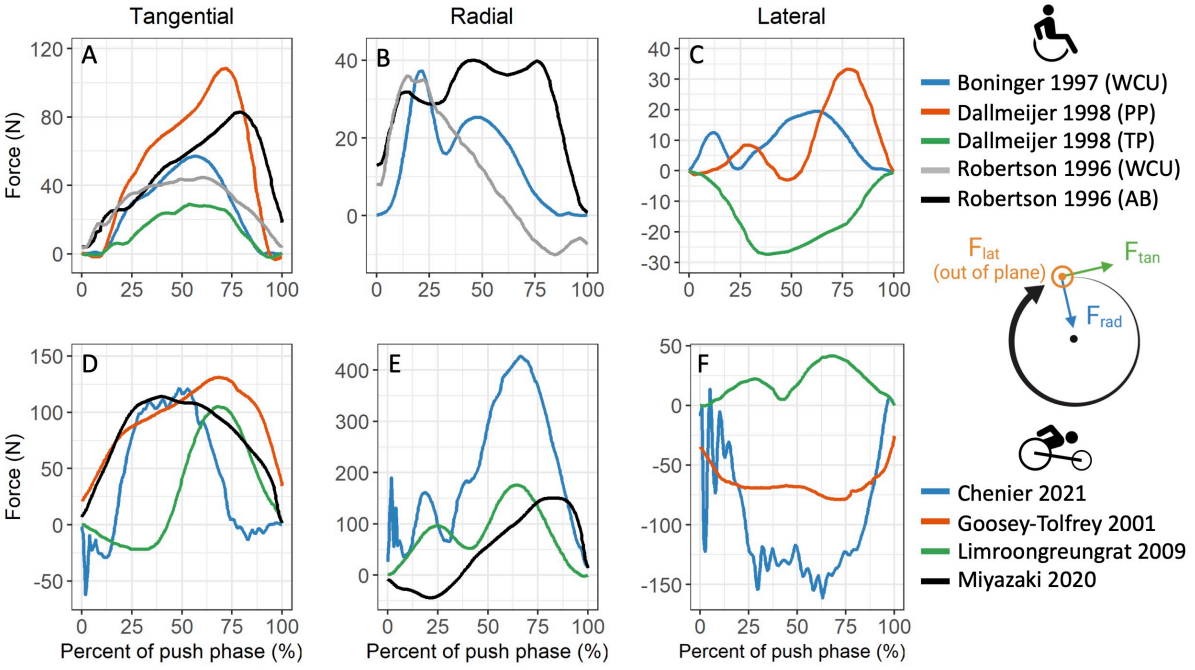

Figure 2: Applied handrim forces (N) during everyday wheelchair propulsion (top row)(Boninger et al., 1997, Dallmeijer et al., 1998, Robertson et al., 1996) and racing wheelchair propulsion (bottom row)(Chénier et al., 2021, Goosey-Tolfrey et al., 2001, Limroongreungrat et al., 2009, Miyazaki et al., 2020) by A,D) tangential component, B,E) radial component, and C,F) lateral component. Force conventions for F_{tan}, F_{rad}, and F_{lat} are on the right. Abbreviations: **PP** (paraplegic subject), **TP** (tetraplegic subject), **AB** (able-bodied subject), **WCU** (wheelchair user).

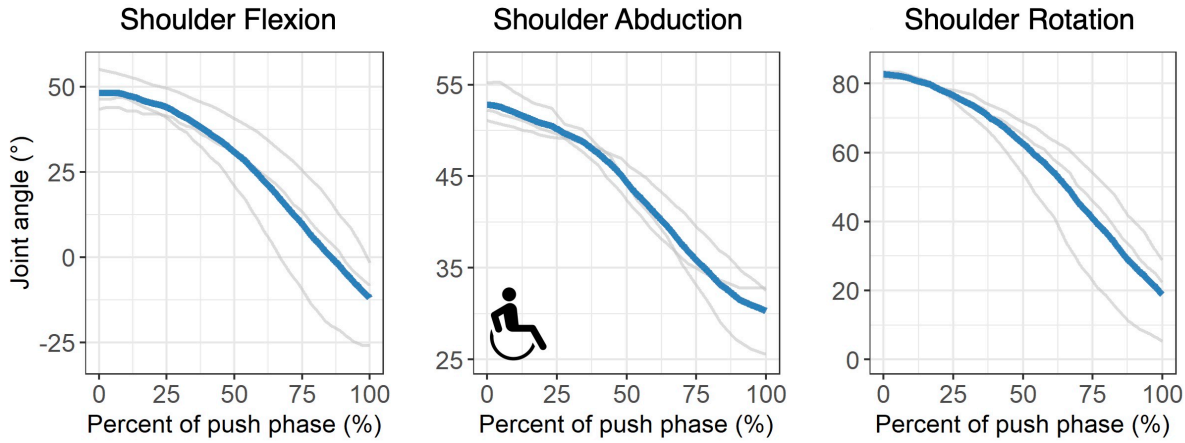

Figure 3: Joint angles (°) during the push phase of everyday wheelchair propulsion, averages in blue(Collinger et al., 2008, Rao et al., 1996).

limited to reports of elbow flexion (Goosey et al., 1998, Goosey and Campbell, 1998).

There are, however, reports of the start and end angles during propulsion (Fig 4)(Wang et al., 1995, Chow et al., 2001, Higgs, 1984, Gehlsen et al., 1990, Goosey-Tolfrey et al., 2001, Miyazaki et al., 2020, Moss et al., 2005, Goosey et al., 1998, Lewis et al., 2018, Dallmeijer et al., 1998, Koontz et al., 2002, Requejo et al., 2015, Boninger et al., 2000, Tsai et al., 2012, Yang et al., 2012). These contact angles are important to quantify because the length of the push phase affects the length of time that the shoulder experiences applied forces (Lewis et al., 2018). In racing propulsion, the mean start angle is 27.8°and the mean end release angle is 197°(Fig 4). The resulting contact angle of 169°indicates that the hand is touching the handrim and transferring forces for almost half of the propulsion cycle. In everyday propulsion, the average push angle is 83°.

Start and end angles vary depending on the handrim propulsion mode with everyday propulsion having a smaller and more precise push phase compared to racing propulsion. The increased variability in the push phase for racing propulsion could be attributed to racing technique (recovery path location, having a tightly closed fist or using the thumb to apply force, etc.) based on personal preference and race length (Higgs, 1984, Chow et al., 2001). While not included in our summary because of the different technique compared to static propulsion, Moss et al.(Moss et al., 2005) reported start and end angles of a sprint start during wheelchair racing.

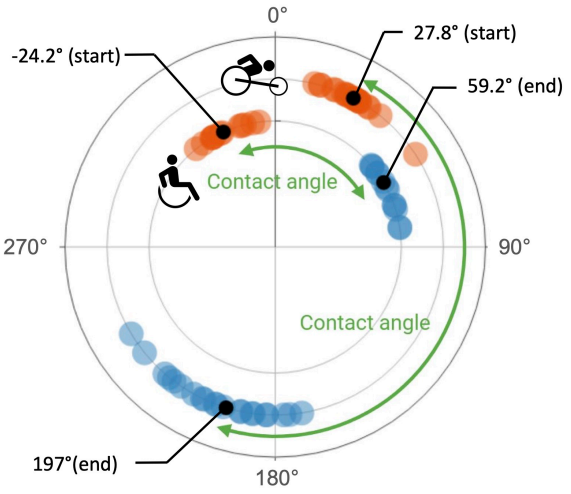

Figure 4: Handrim contact and release angles for racing(Wang et al., 1995, Chow et al., 2001, Higgs, 1984, Gehlsen et al., 1990, Goosey-Tolfrey et al., 2001, Miyazaki et al., 2020, Moss et al., 2005, Goosey et al., 1998, Lewis et al., 2018) and everyday(Dallmeijer et al., 1998, Koontz et al., 2002, Requejo et al., 2015, Boninger et al., 2000, Tsai et al., 2012, Yang et al., 2012) propulsion. Mean angles for each activity are shown in black.

3.5. Implications of handrim wheelchair vs racing propulsion

In general, the maximum applied force components during racing wheelchair propulsion are 1.2-10.7 times larger than those recorded during everyday wheelchair propulsion. This increase is likely due the high speeds and intensities associated with racing. Whether these increased force values may be placing

the shoulder at increased risk for injury remains to be clearly demonstrated. The wide range of force values and profiles across studies points to the need to more fully examine the applied forces of racing propulsion including larger sample sizes with a more consistent method of measuring applied forces.

The lack of shoulder kinematic data during racing prevents a direct comparison to everyday wheelchair usage. However, the start and end angles can also lend insight into changes in propulsion styles. While the longer (2 times the contact angle) push phase in racing compared to everyday propulsion may indicate more time for force transfer (i.e., a decreased rate of loading), and therefore less impact on the shoulder(Boninger et al., 2002), racing propulsion also results in increased forces. Compared to everyday propulsion, racers tend to use their muscle groups differently due to different propulsion styles(Vanlandewijck et al., 2001). The prone/ kneeling body position characteristic of a wheelchair racer requires significant effort from the posterior muscle groups of the upper back during the recovery phase which must work against gravity to initiate the contact phase of propulsion, which is assisted by gravity(Chow et al., 2001, Wang et al., 1995). In contrast, the upright body position of everyday propulsion allows the user to freely position the arms behind the handrim in preparation for contact(Chow and Levy, 2011, Vanlandewijck et al., 2001). However, it is still unclear how the combination of increased forces and larger contact angle during racing propulsion affects shoulder joint loading, and therefore tissue strain and injury risk.

The force transfer during wheelchair propulsion is also dependent on propulsion kinematics: increased shoulder elevation and shoulder rotation are correlated with increased shoulder joint reaction forces during racing propulsion, which is indicative of higher shoulder injury risk(Lewis et al., 2018). Thus, it is important to quantify how the upper arms are moving during wheelchair racing propulsion to optimize force transfer from an injury prevention standpoint.

4. Crank Propulsion

With the introduction of a crank for propulsion, applied forces and movement shift from the period associated with the push angle of propulsion to continuous biomechanical data during a complete propulsion cycle. The gears on a handcycle offer a greater mechanical advantage than handrim propulsion and thus create a more efficient mode of transportation(Dallmeijer et al., 2004). One cycle of the handcycle crank is split into two phases: the pull phase and push phase (Fig 1). During the pull phase, the user is pulling the crank toward themselves; during the push phase, the user is pushing the handle away from the body. One should note that the origin for the angular phases during crank propulsion is different (anterior) than the origin used for handrim propulsion (proximal).

4.1. Attach-unit Handcycling: Crank Kinetics

Three studies have reported continuous applied forces during attach-unit handcycling(VanDrongelen et al., 2011, Kraaijenbrink et al., 2017, 2020), with two studies (VanDrongelen et al., 2011, Kraaijenbrink et al., 2020) reporting all three force components. The tangential force profiles have similar shapes but differ in the magnitude of forces (Fig 5). The largest peak tangential force recorded was 45 Newtons and occurred between 64°and 91°of the cycle (Fig 5).

The transition from push to pull phase is indicated by a local minimum of tangential forces which occurred between 276°and 310°. As rolling resistance increases, tangential forces also increase to maintain speed(Kraaijenbrink et al., 2017). Able-bodied subjects cycling at 1.94 m/s had lower tangential forces(Kraaijenbrink et al., 2017, 2020) than those reported in a subject with paraplegia cycling at 35W (VanDrongelen et al., 2011).

4.2. Recumbent Handcycling: Crank Kinetics

To our knowledge, only one study has reported direct measurements of continuous applied forces during recumbent handcycling (Fig 6A)(Ahlers and Jakobsen, 2016). Ahlers

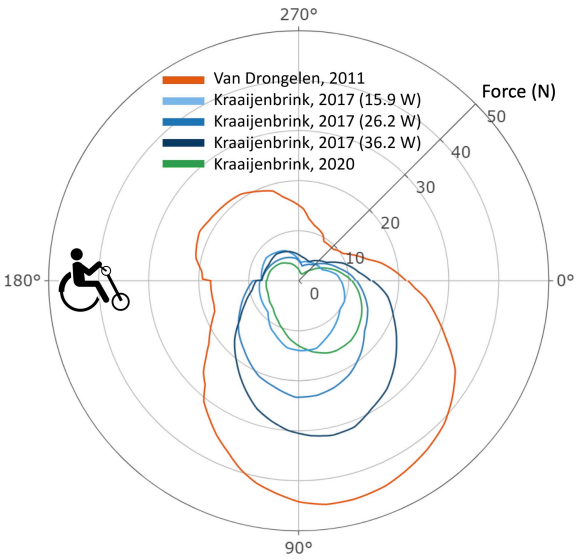

Figure 5: Tangential force (N) during attach-unit handcycling(VanDrongelen et al., 2011, Kraaijenbrink et al., 2017, 2020). The three shades of blue represent crank propulsion for different rolling resistance levels within the same study, measured in Watts. As resistance increases, the shade of blue darkens.

and Jakobsen reported a maximum tangential force of 127 N at 107°in the propulsion cycle, with a pronounced push-pull and pull-push transition at 2°and 199°, respectively. Several studies have investigated the effect of changing either the handcycle configuration (i.e. crank length, backrest angle, crank position, etc.) or the power output during propulsion and reported continuous torque during recumbent handcycling(Quittmann et al., 2018, 2020, Mason et al., 2021, Vegter et al., 2019). This torque data can be used to indirectly calculate the tangential force by dividing the torque at the crank by the crank length. Changes in crank length did not significantly change the applied torque profiles(Mason et al., 2021) (Fig 6B, blue lines). However, torques were sensitive to crank position(Vegter et al., 2019): when the crank is moved closer to the participant, the torque in the push phase increased and torque in the pull phase decreased (Fig 6B). The tangential forces during recumbent handcycling kinetics are also sensitive to changes in power output with maximum force increasing with increasing power.

The location of maximum force across studies was variable (range = 34°- 273°), and could be a result of different levels of handcycling experience, handcycle design, participant demographics, and different methodologies in collecting force data. The location of the push-pull transition (291°-2°) and pull-push transition (132°-199°) (Fig 1, top right), defined as the location of minimum applied force, were more consistent across studies though studies investigating the effect of power (Fig 6C) did not report a clear transition point. Compared to attach unit handcycling, the push-pull transition occurs later in the propulsion cycle. Notably, direct measures of the tangential force (Fig 6A) had similar force profiles to that recorded during attach unit handcycling, with the maximum tangential force occurring at the bottom of the propulsion cycle (Fig 5). It is possible that with more consistent data collection methods across recumbent and attach-unit handcycling, a clearer tangential force curve would emerge.

4.3. Attach-unit Handcycling: Kinematics

We did not find any studies that reported continuous joint angles during attach-unit handcycling. Faupin and Gorce reported the maximum and minimum shoulder angles for one able-bodied participant and one participant with paraplegia during 70 rpm handcycling(Faupin and Gorce, 2008). They reported a 63, 19, and 11 degree range of motion for shoulder flexion, abduction, and rotation, respectively, for the able-bodied participant. The range of motion for the subject with paraplegia was greater than the able-bodied subject, with 71, 23, and 17 degree ranges of motion for shoulder flexion, abduction, and rotation, respectively.

4.4. Recumbent Handcycling: Kinematics

In contrast to attach-unit handcycling, continuous kinematic data during recumbent handcycling has been reported(Faupin et al., 2010, Mason et al., 2021, Quittmann et al., 2018, 2020, Stone et al., 2019, Chiodi, 2016). Handcycling begins with the shoulder in abduction after which it continues to abduct by 31°, followed by adduction to 10°(Fig 7A). An average maximum abduction of 31°occurs at 199°in the propulsion cycle. There is a slight

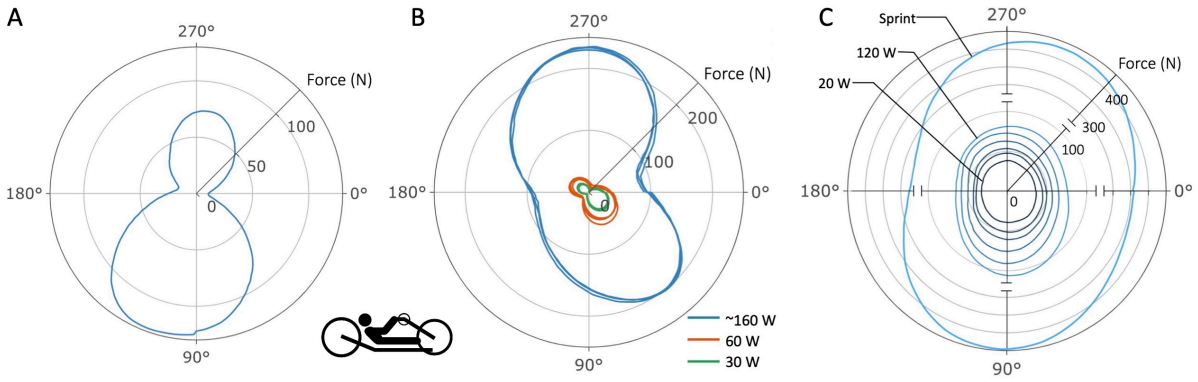

Figure 6: Tangential applied force (F_{tan}) (N) during recumbent handcycling. Studies examining A) F_{tan} measured directly using a strain gauge-instrumented handle, self-selected speed(Jakobsen and Ahlers, 2016), B) changes in handcycle configuration (changes in crank length shown in blue(Mason et al., 2021), and changes in crank fore-aft position, as a percentage of arm length, shown in orange and green(Vegter et al., 2019)) and C) changes in power (20-120W) (Quittmann et al., 2018) and sprinting (Quittmann et al., 2020).

increase in shoulder abduction to 39°with an increase in power output. Shoulder flexion exhibits two peaks during recumbent handcycling: initially the shoulder is flexed to 27°and then extends to -19°followed by a return to flexion which peaks at 300°towards the end of the propulsion cycle (Fig 7B).

The variation between studies in shoulder abduction and flexion was less than the variation in shoulder internal / external rotation (Fig 7C). Studies that used acromion marker clusters(Warner et al., 2012) to track scapular movement reported a wider variation in shoulder rotation, from -10°to 45°(Stone et al., 2019, Mason et al., 2021) than those that did not use an acromion cluster (10°to 25°,(Quittmann et al., 2018, Faupin et al., 2010)).

4.5. Implications for attach unit vs recumbent handcycling

During sprinting, the tangential applied forces reach a maximum of 447 N, which is more than ten times larger than the maximum tangential forces reported during attach-unit handcycling. When athletes train at increased speeds and power outputs, it is reasonable to suggest that these increased external forces will result in increased loads at the shoulder. The question remains as to which power or speed levels, and for how long, are acceptable to avoid overuse injuries common in wheelchair athletes. Additionally, only continuous F_{tan} data was available in the literature for recumbent handcycling. While F_{tan} is the majority of the total applied force during attach-unit handcycling, an understand-

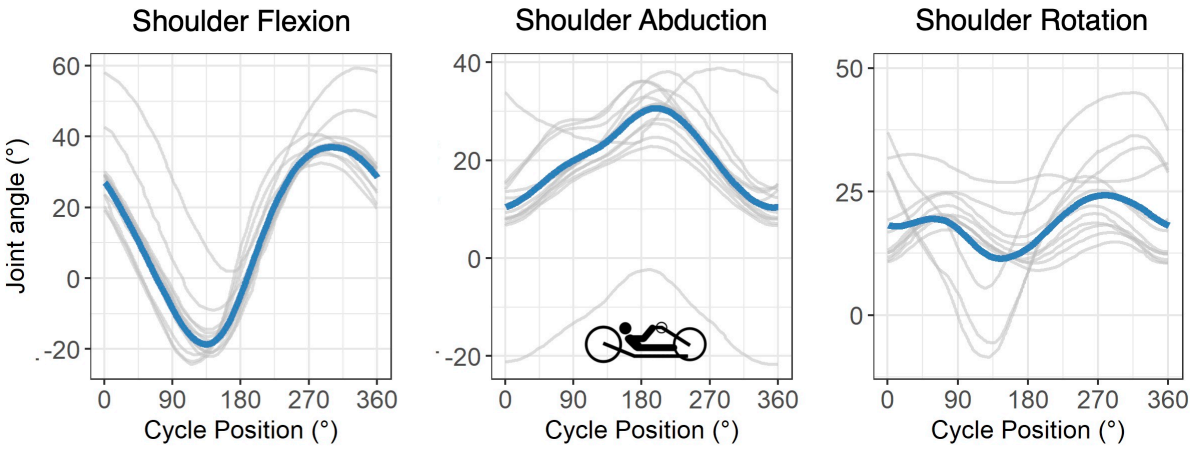

Figure 7: Recumbent handcycling joint angles (°), averages in blue.(Faupin et al., 2010, Mason et al., 2021, Quittmann et al., 2018, 2020, Stone et al., 2019, Chiodi, 2016)

ing of the effect of recumbent handcycle configurations and power on the remaining radial and lateral components is missing. Changes in applied forces for all three directions are important for modeling the upper extremities and understanding musculoskeletal loads during any activity including recumbent handcycling (Bregman et al., 2009).

Kinematic differences are also important: the elevated positions associated with increased power could be a source of increased injury risk(Cools et al., 2015). Arnet et al. found that a more inclined backrest position (more recumbent) leads to higher shoulder loads in attach-unit handcycling(Arnet, 2012). While the impact of shoulder rotation on shoulder soft tissue strain has not been quantified for recumbent handcycling, higher internal rotation was identified as a risk factor during weight bearing activities for shoulder pain in WCUs(Nawoczenski et al., 2012). More data is needed to identify potential stages during crank propulsion when the load on the shoulder is highest in order to optimize training protocols for reduced injury risk.

A more thorough investigation of the three-dimensional shoulder loads during recumbent handcycling using models specific to WCUs could provide insight into injury risk and prevention techniques, especially at the higher speeds experienced during recumbent handcycling races and exercise.

5. Conclusion

Upper extremity injuries, lack of exercise, and high rates of CVD in WCUs represent a multi-factorial problem which exert a clear burden on both individuals and society. A better understanding of upper-limb kinetics and kinematics during propulsion can lend insight into joint loading, and therefore injury risk, experienced by WCUs during both handrim and crank propulsion. In general, the applied hand forces are larger for both athletic propulsion modes (racing wheelchair propulsion and recumbent handcycling) and could be indicative of increased shoulder loading. While this data is a promising start to characterizing the biomechanics of common propulsion modes in WCUs, there is still a need to better understand the nature of shoulder loads.

One limitation encountered in this review was the variability in the reporting of results. Here, we summarized shoulder angles in the flexion/abduction/rotation angle convention (Fig 1) as this is the set of rotations most consistently reported in the literature. However, in 2005, the ISB recommended using an alternative set of rotation angles (plane of elevation/elevation/rotation) to avoid confusion between biomechanical and clinical definitions of "abduction"(Wu et al., 2005, Anglin and Wyss, 2000). A standardized approach to shoulder angles would allow for more comparison between papers that currently report different angle rotation conventions.

Kinematic and external load data are useful for such data can be used with upper limb rigid-dynamics models to calculate joint torques and accelerations, joint contact forces, and muscle forces. There is still a need to more completely characterize shoulder joint angles during racing wheelchair propulsion and continuous three-dimensional forces during recumbent handcycling. Once these propulsion styles are better understood, we can develop predictive models for coaching, training, and physical therapy to reduce shoulder injury risk and increase the quality of life for WCUs.

References

Ahlers, F. H. and Jakobsen, L. (2016). Biomechanical analysis of hand cycling propulsion movement : A musculoskeletal modelling approach.

Alm, M., Saraste, H., and Norrbrink, C. (2008). Shoulder pain in persons with thoracic spinal cord injury: Prevalence and characteristics. *Journal of Rehabilitation Medicine*, 40:277–283.

Anglin, C. and Wyss, U. (2000). Review of arm motion analyses. *Proceedings of the Institution of Mechanical Engineers, Part H: Journal of Engineering in Medicine*, 214(5):541–555.

Arnet, U. (2012). *Handcycling : a biophysical analysis*.

Barber, D. B. and Gall, M. D. (1991). Osteonecrosis: An overuse injury of the shoulder in paraplegia: Case report. *Paraplegia*, 29:423–426.

Barry, W., Andre, J. R. S., Evans, C. T., Sabharwal, S., Miskevics, S., Weaver, F. M., and Smith, B. M. (2013). Hypertension and antihypertensive treatment in veterans with spinal cord injury and disorders. *Spinal Cord*, 51:109–115.

Bayley, J. C., Cochran, T. P., and Sledge, C. B. (1987). The weight-bearing shoulder. the impingement syndrome in paraplegics. *Journal of Bone and Joint Surgery - Series A*, 69:676–678.

Blauwet, C. and Willick, S. E. (2012). The paralympic movement: Using sports to promote health, disability rights, and social integration for athletes with disabilities. *PM and R*, 4:851–856.

Boninger, M. L., Baldwin, M., Cooper, R. A., Koontz, A., and Chan, L. (2000). Manual wheelchair pushrim biomechanics and axle position. *Archives of Physical Medicine and Rehabilitation*, 81:608–613.

Boninger, M. L., Cooper, R. A., Robertson, R. N., and Shimada, S. D. (1997). Three-dimensional pushrim forces during two speeds of wheelchair propulsion. *American Journal of Physical Medicine and Rehabilitation*, 76.

Boninger, M. L., Cooper, R. A., Shimada, S. D., and Rudy, T. E. (1998). Shoulder and elbow motion during two speeds of wheelchair propulsion: a description using a local coordinate system. *Spinal Cord*, pages 418–426.

Boninger, M. L., Souza, A. L., Cooper, R. A., Fitzgerald, S. G., Koontz, A. M., and Fay, B. T. (2002). Propulsion patterns and pushrim biomechanics in manual wheelchair propulsion. *Archives of Physical Medicine and Rehabilitation*, 83:718–723.

Bregman, D. J., van Drongelen, S., and Veeger, H. E. (2009). Is effective force application in handrim wheelchair propulsion also efficient? *Clinical Biomechanics*, 24:13–19.

Brose, S. W., Boninger, M. L., Fullerton, B., McCann, T., Collinger, J. L., Impink, B. G., and Dyson-Hudson, T. A. (2008). Shoulder ultrasound abnormalities, physical examination findings, and pain in manual wheelchair users with spinal cord injury. *Archives of Physical Medicine and Rehabilitation*, 89:2086–2093.

Burnham, R. S., May, L., Nelson, E., Steadward, R., and Reid, D. C. (1993). Shoulder pain in wheelchair athletes: The role of muscle imbalance.

Chiodi, E. (2016). A biomechanical model of the upper limb applied to the handcycling.

Chow, J. W. and Levy, C. E. (2011). Wheelchair propulsion biomechanics and wheelers' quality of life: An exploratory review. *Disability and Rehabilitation: Assistive Technology*, 6:365–377.

Chow, J. W., Millikan, T. A., Carlton, L. G., Morse, M. I., and sik Chae, W. (2001). Biomechanical comparison of two racing wheelchair propulsion techniques. *Medicine and science in sports and exercise*, pages 476–484.

Chénier, F., Pelland-Leblanc, J. P., Parrinello, A., Marquis, E., and Rancourt, D. (2021). A high sample rate, wireless instrumented wheel for measuring 3d pushrim kinetics of a racing wheelchair. *Medical Engineering and Physics*, 87:30–37.

Collinger, J. L., Boninger, M. L., Koontz, A. M., Price, R., Sisto, S. A., Tolerico, M. L., and Cooper, R. A. (2008). Shoulder biomechanics during the push phase of wheelchair propulsion: A multisite study of persons with paraplegia. *Archives of Physical Medicine and Rehabilitation*, 89:667–676.

Cools, A. M., Johansson, F. R., Borms, D., and Maenhout, A. (2015). Prevention of shoulder injuries in overhead athletes: A science-based approach. *Brazilian Journal of Physical Therapy*, 19:331–339.

Cooper, R. A. and Luigi, A. J. D. (2014). Adaptive sports technology and biomechanics: Wheelchairs. *PM and R*, 6:31–39.

Curtis, K. A. and Dillon, D. A. (1985). Survey of wheelchair athletic injuries: Common patterns and prevention.

Dallmeijer, A. J., der Woude, L. H. V., Veeger, H. E., and Hollander, A. P. (1998). Effectiveness of force application in manual wheelchair propulsion in persons with spinal cord injuries. *American Journal of Physical Medicine and Rehabilitation*, 77.

Dallmeijer, A. J., Zentgraaff, I. D., Zijp, N. I., and Woude, L. H. V. D. (2004). Submaximal physical strain and peak performance in handcycling versus handrim wheelchair propulsion. *Spinal Cord*, 42:91–98.

Dalyan, M., Cardenas, D. D., and Gerard, B. (1999). Upper extremity pain after spinal cord injury.

Faber, H., Soest, A. J. V., and Kistemaker, D. A. (2018). Inverse dynamics of mechanical multibody systems: An improved algorithm that ensures consistency between kinematics and external forces. *PLoS ONE*, 13:1–16.

Faupin, A. and Gorce, P. (2008). The effects of crank adjustments on handbike propulsion: A kinematic model approach. *International Journal of Industrial Ergonomics*, 38:577–583.

Faupin, A., Gorce, P., Watelain, E., Meyer, C., and Thevenon, A. (2010). A biomechanical analysis of handcycling: A case study. *Journal of Applied Biomechanics*, 26:240–245.

Finley, M. A., Rasch, E. K., Keyser, R. E., and Rodgers, M. M. (2004). The biomechanics of wheelchair propulsion in individuals with and without upper-limb impairment.

Gater, D. R., Farkas, G. J., Berg, A. S., and Castillo, C. (2019). Prevalence of metabolic syndrome in

veterans with spinal cord injury. *Journal of Spinal Cord Medicine*, 42:86–93.

Gehlsen, G. M., Davis, R. W., and Bahamonde, R. (1990). Intermittent velocity and wheelchair performance characteristics. *Adapted Physical Activity Quarterly*, 7:219–230.

Gill, T. K., Shanahan, E. M., Allison, D., Alcorn, D., and Hill, C. L. (2014). Prevalence of abnormalities on shoulder mri in symptomatic and asymptomatic older adults. *International Journal of Rheumatic Diseases*, 17:863–871.

Goosey, V. L. and Campbell, I. G. (1998). Symmetry of the elbow kinematics during racing wheelchair propulsion. *Ergonomics*, 41:1810–1820.

Goosey, V. L., Campbell, I. G., and Fowler, N. E. (1998). The relationship between three-dimensional wheelchair propulsion techniques and pushing economy. *Journal of Applied Biomechanics*, 14:412–427.

Goosey-Tolfrey, V. L., Fowler, N. E., Campbell, I. G., and Iwnicki, S. D. (2001). A kinetic analysis of trained wheelchair racers during two speeds of propulsion. *Medical Engineering and Physics*, 23:259–266.

Gorgey, A. S. (2014). Exercise awareness and barriers after spinal cord injury. *World Journal of Orthopaedics*, 5:158–162.

Hansen, R. K., Larsen, R. G., Laessoe, U., Samani, A., and Cowan, R. E. (2021). Physical activity barriers in danish manual wheelchair users: A cross-sectional study. *Archives of physical medicine and rehabilitation*, 102(4):687–693.

Heyward, O. W., Vegter, R. J., Groot, S. D., and Woude, L. H. V. D. (2017). Shoulder complaints in wheelchair athletes: A systematic review. *PLoS ONE*, 12:1–20.

Higgs, C. (1984). Propulsion of racing wheelchairs. *Sports and disabled athletes*, 1:165–172.

Hinrichs, T., Lay, V., Arnet, U., Eriks-Hoogland, I., Koch, H. G., Rantanen, T., Reinhardt, J. D., Brinkhof, M. W., Dériaz, O., Baumberger, M., Gmünder, H. P., Curt, A., Schubert, M., Hund-Georgiadis, M., Hug, K., Koch, H. G., Styger, U., Landolt, H., Koch, H., Brach, M., Stucki, G., Brinkhof, M., and Thyrian, C. (2016). Age-related variation in mobility independence among wheelchair users with spinal cord injury: A cross-sectional study. *Journal of Spinal Cord Medicine*, 39:180–189.

Inoue, A., Chosa, E., Goto, K., and Tajima, N. (2013). Nonlinear stress analysis of the supraspinatus tendon using three-dimensional finite element analysis. *Knee Surgery, Sports Traumatology, Arthroscopy*, 21:1151–1157.

Jahanian, O., Straaten, M. G. V., Goodwin, B. M., Lennon, R. J., Barlow, J. D., Murthy, N. S., and Morrow, M. M. (2020). Shoulder magnetic resonance imaging findings in manual wheelchair users with spinal cord injury. *Journal of Spinal Cord Medicine*, 0:1–11.

Jakobsen, L. and Ahlers, F. H. (2016). Development of a wireless crank moment measurement-system for a handbike: Initial results of propulsion kinetics.

Karmarkar, A. M., Dicianno, B. E., Cooper, R., Collins, D. M., Matthews, J. T., Koontz, A., Teodorski, E. E., and Cooper, R. A. (2011). Demographic profile of older adults using wheeled mobility devices. *Journal of Aging Research*, 2011.

Kehn, M. and Kroll, T. (2009). Staying physically active after spinal cord injury: A qualitative exploration of barriers and facilitators to exercise participation. *BMC Public Health*, 9:1–11.

Koontz, A. M., Cooper, R. A., Boninger, M. L., Souza, A. L., and Fay, B. T. (2002). Shoulder kinematics and kinetics during two speeds of wheelchair propulsion.

Kraaijenbrink, C., Vegter, R. J., Hensen, A. H., Wagner, H., and Woude, L. H. V. D. (2017). Different cadences and resistances in submaximal synchronous handcycling in able-bodied men: Effects on efficiency and force application. *PLoS ONE*, 12.

Kraaijenbrink, C., Vegter, R. J., Hensen, A. H., Wagner, H., and Woude, L. H. V. D. (2020). Biomechanical and physiological differences between synchronous and asynchronous low intensity handcycling during practice-based learning in able-bodied men. *Journal of NeuroEngineering and Rehabilitation*, 17.

Lal, S. (1998). Premature degenerative shoulder changes in spinal cord injury patients. *Spinal Cord*, 36:186–189.

Lewis, A. R., Phillips, E. J., Robertson, W. S. P., Grimshaw, P. N., and Portus, M. (2018). Injury prevention of elite wheelchair racing athletes using simulation approaches. *Proceedings*, 2:255.

Limroongreungrat, W., Wang, Y. T., Chang, L. S., Geil, M. D., and Johnson, J. T. (2009). An instrumented wheel system for measuring 3-d pushrim kinetics during racing wheelchair propulsion. *Research in Sports Medicine*, 17:182–194.

Martinez, R., Assila, N., Goubault, E., and Begon, M. (2020). Sex differences in upper limb musculoskeletal biomechanics during a lifting task. *Applied ergonomics*, 86:103106.

Mason, B. S., Stone, B., Warner, M. B., and Goosey-Tolfrey, V. L. (2021). Crank length alters kinematics and kinetics, yet not the economy of recumbent handcyclists at constant handgrip speeds. *Scandinavian Journal of Medicine and Science in Sports*, 31:388–397.

Miyazaki, Y., Iida, K., Nakashima, M., Maruyama, T., and Yamanobe, K. (2020). Measurement of pushrim forces during racing wheelchair propulsion using a novel attachable force sensor system. *Proceedings of the Institution of Mechanical Engineers, Part P: Journal of Sports Engineering and Technology*.

Moss, A. D., Fowler, N. E., and Goosey-Tolfrey, V. L. (2005). The intra-push velocity profile of the overground racing wheelchair sprint start. *Journal of Biomechanics*, 38:15–22.

Nawoczenski, D. A., Riek, L. M., Greco, L., Staiti, K., and Ludewig, P. M. (2012). Effect of shoulder pain on shoulder kinematics during weight-bearing tasks in persons with spinal cord injury. *Archives of Physical Medicine and Rehabilitation*, 93:1421–1430.

Quittmann, O. J., Abel, T., Albracht, K., and Strüder,

H. K. (2020). Biomechanics of all-out handcycling exercise: kinetics, kinematics and muscular activity of a 15-s sprint test in able-bodied participants. *Sports Biomechanics*.

Quittmann, O. J., Meskemper, J., Abel, T., Albracht, K., Foitschik, T., Rojas-Vega, S., and Strüder, H. K. (2018). Kinematics and kinetics of handcycling propulsion at increasing workloads in able-bodied subjects. *Sports Engineering*, 21:283–294.

Rao, S. S., Bontrager, E. L., Gronley, J. K., Newsam, C. J., and Perry, J. (1996). Three-dimensional kinematics of wheelchair propulsion. *IEEE Transactions on Rehabilitation Engineering*, 4:152–160.

Redepenning, D. H., Ludewig, P. M., and Looft, J. M. (2020). Finite element analysis of the rotator cuff: A systematic review.

Requejo, P. S., Mulroy, S. J., Ruparel, P., Hatchett, P. E., Haubert, L. L., Eberly, V. J., and Gronley, J. A. K. (2015). Relationship between hand contact angle and shoulder loading during manual wheelchair propulsion by individuals with paraplegia. *Topics in Spinal Cord Injury Rehabilitation*, 21:313–324.

Robertson, R. N., Boninger, M. L., Cooper, R. A., and Shimada, S. D. (1996). Pushrim forces and joint kinetics during wheelchair propulsion.

Stone, B., Mason, B. S., Warner, M. B., and Goosey-Tolfrey, V. L. (2019). Shoulder and thorax kinematics contribute to increased power output of competitive handcyclists. *Scandinavian Journal of Medicine and Science in Sports*, 29:843–853.

Subbarao, J. V., Klopfstein, J., and Turpin, R. (1995). Prevalence and impact of wrist and shoulder pain in patients with spinal cord injury. *The journal of spinal cord medicine*, 18:9–13.

Taylor, D. M. (2018). Americans with disabilities: 2014. *Current Population Reports*, pages 1–32.

Tsai, C. Y., Lin, C. J., Huang, Y. C., Lin, P. C., and Su, F. C. (2012). The effects of rear-wheel camber on the kinematics of upper extremity during wheelchair propulsion. *BioMedical Engineering Online*, 11.

VanDrongelen, S., van den Berg, J., Arnet, U., Veeger, D. J., and van der Woude, L. H. (2011). Development and validity of an instrumented handbike: Initial results of propulsion kinetics. *Medical Engineering and Physics*, 33:1167–1173.

Vanlandewijck, Y., Theisen, D., and Daly, D. (2001). Wheelchair propulsion biomechanics. *Sports Medicine*, 31:339–367.

Veeger, H. E. J., Rozendaal, L. A., and Helm, F. C. T. V. D. (2002). Load on the shoulder in low intensity wheelchair propulsion. *Clinical Biomechanics*, 17:211–218.

Vegter, R. J., Mason, B. S., Sporrel, B., Stone, B., van der Woude, L. H., and Goosey-Tolfrey, V. L. (2019). Crank fore-aft position alters the distribution of work over the push and pull phase during synchronous recumbent handcycling of able-bodied participants. *PLoS ONE*, 14:1–14.

Wang, Y. T., Deutsch, H., Morse, M., Hedrick, B., and Millikan, T. (1995). Three-dimensional kinematics of wheelchair propulsion across racing speeds. *Adapted Physical Activity Quarterly*, 12:78–89.

Warner, M. B., Chappell, P. H., and Stokes, M. J. (2012). Measuring scapular kinematics during arm lowering using the acromion marker cluster. *Human Movement Science*, 31:386–396.

Wu, G., Helm, F. C. V. D., Veeger, H. E., Makhsous, M., Roy, P. V., Anglin, C., Nagels, J., Karduna, A. R., McQuade, K., Wang, X., Werner, F. W., and Buchholz, B. (2005). Isb recommendation on definitions of joint coordinate systems of various joints for the reporting of human joint motion - part ii: Shoulder, elbow, wrist and hand. *Journal of Biomechanics*, 38:981–992.

Wu, W., Lee, P. V., Bryant, A. L., Galea, M., and Ackland, D. C. (2016). Subject-specific musculoskeletal modeling in the evaluation of shoulder muscle and joint function. *Journal of Biomechanics*, 49:3626–3634.

Yang, Y. S., Koontz, A. M., Yeh, S. J., and Chang, J. J. (2012). Effect of backrest height on wheelchair propulsion biomechanics for level and uphill conditions. *Archives of Physical Medicine and Rehabilitation*, 93:654–659.

Some figures created with BioRender.com